Cobalt multilayers on diamond surfaces: An *ab initio* study

Bernd Stärk,* Peter Krüger, and Johannes Pollmann
Institut für Festkörpertheorie, Westfälische Wilhelms-Universität Münster, D-48149 Münster, Germany
(Received 29 May 2009; revised manuscript received 22 October 2009; published 13 January 2010)

Structural, electronic, and magnetic properties of particular metal-semiconductor hybrid systems are investigated employing spin-density-functional theory within generalized gradient approximation. They consist of one up to six monolayers of cobalt on (111) and (001) surfaces of diamond and are characterized by a very small lattice mismatch of the constituents. For monolayer coverage, the Co atoms adsorb in *on top* sites on the C(111) surface while they adsorb in symmetric *bridge* sites on the C(001) surface. Strong covalent bonds are formed between the Co 3*d* and C 2*p* orbitals which saturate all surface dangling bonds in each case. The *pd* bonds give rise to characteristic bonding and antibonding bands which exhibit no significant spin splitting. As a result, the magnetic moment of the Co atoms on the interface layer is considerably quenched. The magnetic moment of $0.96\mu_B$ per Co atom for one Co adlayer on C(111) turns out to be strongly reduced with respect to $1.76\mu_B$ for the top layer atoms of a Co(0001) surface or $1.87\mu_B$ for a free-standing hexagonal Co monolayer. Further Co adlayers lead to an increase in the magnetization rapidly approaching $1.19\mu_B$ at the Co interface and $1.77\mu_B$ at the Co surface layer. For one Co adlayer on C(001), where each Co atom forms two *pd* bonds with the substrate, the magnetic moment per Co atom is even reduced to $0.42\mu_B$, as compared to $1.92\mu_B$ for the top layer atoms of a Co(001) surface or $2.05\mu_B$ for a free-standing cubic Co monolayer. For six Co adlayers on C(001) the magnetic moment turns out to be $0.91\mu_B$ at the interface and $1.92\mu_B$ at the surface layer. For both types of hybrid systems the spin polarization at the Co-C interface depends sensitively on the number of Co adlayers. For several systems it amounts to about 60% at the Fermi level.

DOI: 10.1103/PhysRevB.81.035321 PACS number(s): 73.20.At, 75.70.Ak, 75.70.Cn, 68.43.Fg

I. INTRODUCTION

In recent years there has been an ever increasing interest in the development and understanding of metal-semiconductor hybrid systems. They may feature novel functionalities which are not feasible with metals or semiconductors alone combining, e.g., the high conductivity and spin polarization of ferromagnets with the controllability of semiconductors.[1] A possible application for this new class of systems is the spin field-effect transistor as described by Datta and Das.[2] The basic idea of this device is to generate spin-polarized currents in a ferromagnetic source and to transfer them into the gate via ballistic transport. Since the gate is usually made of a semiconducting material a thorough understanding of the interface in metal-semiconductor hybrid systems is of paramount importance.

Over the past decade a large number of such hybrid systems has been investigated. For example, ferromagnetic semiconductors such as $In_{1-x}Mn_xAs$ compounds on III-V semiconductors[1] as well as ultrathin films of ferromagnetic MnSi on Si(001) (Ref. 3) have been explored. Motivated by scanning-tunneling microscopy experiments, Sacharow *et al.*[4] have theoretically analyzed structural, electronic, and magnetic properties of a Fe monolayer on InAs(110). The authors find that the relaxation of the substrate is completely lifted due to the chemisorbed Fe adlayer resulting in large magnetic moments for the Fe atoms. High relative spin polarizations of 80% at the Fe side and 60% at the InAs side of the interface are found at the Fermi energy E_F. As another example, spin injection through a Fe-InAs interface has been studied by Zwierzycki *et al.*[5]

Metal-semiconductor hybrid systems suitable for applications should have a good structural compatibility of their constituents since a large lattice mismatch leads to diffusive transport processes, as has been shown previously.[6] The latter quickly destroy the spin polarization of the currents induced by the source. Therefore, it is highly desirable to identify systems which are not susceptible to such limitations.

To this end, we suggest hybrid systems consisting of Co multilayers adsorbed on (111) or (001) diamond surfaces. They are almost ideally lattice matched. The related high structural compatibility of graphene on Co surfaces has been appreciated earlier by Karpan *et al.*[7] Bulk Co crystallizes in hcp and fcc structure depending on temperature and pressure. At room temperature, the hcp structure is the standard modification which converts into the fcc structure when temperatures of $T>695$ K are applied. Experimentally it is possible to stabilize fcc Co at room temperature by growing $Co_{0.92}Fe_{0.08}$ alloys.[8] Co nanoparticles, on the other hand, have fcc structure as their standard modification already at room temperature.[9] The experimental lattice constants[10] of Co are $a=3.54$ Å for the fcc and $a=2.51$ Å and $c=4.07$ Å for the hcp structure. These lattice constants show an almost perfect matching with the surface lattice constants[11] of $a_{fcc}=3.57$ Å for C(001) and $a_{hex}=a_{fcc}/\sqrt{2}=2.52$ Å for C(111). Therefore, Co-C hybrid systems show a very small mismatch of the surface lattice constants of less than 1%. To be suitable for the aforementioned technological purposes, these hybrid systems have to feature a large structural stability and a high degree of spin polarization at E_F. Almost complete spin polarization in bulk samples is not a sufficient prerequisite because the interface may significantly change the magnetic properties.

In this paper we scrutinize this aspect by investigating the physical properties of thin Co adlayers on C(111) and C(001) surfaces. In particular, we study structural, electronic, and

magnetic properties of one up to six monolayers of Co adsorbed on these surfaces. In addition, the spin polarization of the systems at E_F is addressed.

The paper is organized as follows. In Sec. II we briefly discuss the calculational methodology employed. In Sec. III A we present the optimal atomic configurations and related relaxations in the hybrid systems for varying numbers of adsorbate layers. Subsequently, we address the electronic properties and their implications for the magnetic behavior of the hybrid systems in Sec. III B. We conclude the paper with a brief summary in Sec. IV.

II. METHODOLOGY

Our calculations are carried out in the framework of spin-density-functional theory employing the generalized gradient approximation[12] for exchange and correlation. We use norm-conserving pseudopotentials in the Kleinman-Bylander form,[13] generated according to the prescription of Hamann.[14] Nonlinear core corrections[15] are included for a proper representation of structural and magnetic properties. The wave functions are expanded in a basis set of atom-centered Gaussian orbitals of s, p, d and s^* symmetry with appropriate decay constants.[16] Since the Co pseudopotentials are rather hard, strongly localized orbitals are needed for an appropriate description of the Co wave functions. For the same reason a fine real-space mesh with some 4000 points per Å^3 is needed to represent the charge density. To evaluate the charge density as well as the potential matrix elements we resort to the very efficient algorithms presented in Ref. 17.

Integrations over the Brillouin zone are performed using special **k**-point sets according to the prescription of Monkhorst and Pack.[18] To obtain reliable results for spin polarization as well as magnetization a precise sampling of the Fermi surface is mandatory. In this work we use a $20\times20\times1$ **k**-point grid together with a Gaussian broadening of the density of states by 60 meV.

The absolute spin polarization per layer unit cell at E_F is given by

$$\zeta_\nu^{\mathrm{abs}}(E_F) = N_\nu^{\uparrow}(E_F) - N_\nu^{\downarrow}(E_F) \tag{1}$$

while the relative spin polarization per layer unit cell at E_F is given by

$$\zeta_\nu(E_F) = [N_\nu^{\uparrow}(E_F) - N_\nu^{\downarrow}(E_F)]/[N_\nu^{\uparrow}(E_F) + N_\nu^{\downarrow}(E_F)], \tag{2}$$

where $N_\nu^{\uparrow}$ and $N_\nu^{\downarrow}$ are the densities of states (DOSs) for spin-up (majority) and spin-down (minority) electrons on layer ν, respectively. Atom- and spin-resolved densities of states $N_\nu^{\sigma}(E)$ and magnetic moments μ_ν^{σ} are directly obtained via a Mulliken analysis.

The hybrid systems are treated within the standard supercell approach using slabs containing six C substrate layers and up to six Co adlayers as well as a vacuum of 12 Å between the slabs. To prevent unphysical states originating from the bottom of the slabs we saturate the free bonds of the lower C surface atoms with hydrogen atoms.[16] In the total-energy minimization calculations the lower two C layers of the substrates and the saturating hydrogen layer are fixed in their respective bulk positions while all other atoms are allowed to relax until all forces are smaller than 1 mRy/a_B.

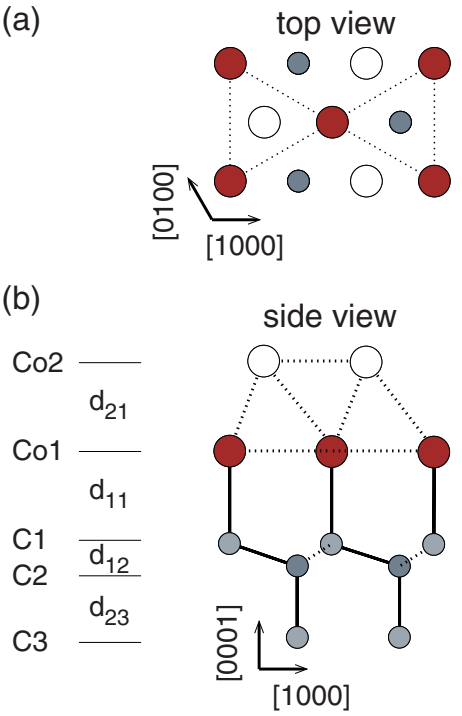

FIG. 1. (Color online) Top and side view of one and two Co adlayers on the C(111) surface (see text). Large filled (red) circles mark Co atoms on the first and large open circles mark Co atoms on the second adlayer. Small (blue) circles indicate C substrate atoms. Full lines represent covalent sp^3 or pd bonds parallel to the drawing plane while dashed lines represent sp^3 bonds that form an angle with the drawing plane or metallic dd bonds. In the top view only dd bonds between Co atoms on the first adlayer are indicated by dashed lines.

III. RESULTS

A. Structural properties

Our lattice constants for hcp and fcc Co are $a=2.52$ Å and $a=3.57$ Å, slightly overestimating the experimental lattice constants by 0.4% and 0.8%, respectively. For diamond we obtain, in full agreement with experiment, a bulk lattice constant of $a=3.57$ Å. Our theoretical lattice constants of cobalt and diamond thus match and can directly be used for all hybrid systems studied in this work, therefore.

In the following, we refer to hybrid systems containing n layers of Co adsorbed on a C(111) substrate surface as n-Co:C(111) systems. We discuss their structural properties starting out with one Co adlayer. Two conceivable structures have been investigated. The filled circles in Fig. 1 show a top and side view of the energetically most favorable adsorption configuration. The Co atoms are located above the C atoms of the topmost C(111) layer in *on top* (OT) position. In this configuration all substrate dangling bonds become saturated by the formation of one strong covalent Co-C bond per unit cell whose length of 1.97 Å is close to the sum of the covalent radii of C (0.77 Å) and Co (1.16 Å). Co adsorption in

TABLE I. Interlayer distances d_{ij} (in Å) between neighboring atomic layers i and j for n-Co:C(111) hybrid systems with n from 1 to 6. In each case, d_{11} is the distance between the Co and C layer at the interface. The rows above and below d_{11} refer to interlayer distances of Co and C layers, respectively. For reference, the first five interlayer distances between the six top layers of a Co(0001) surface are included in the last column.

	1	2	3	4	5	6	Co(0001)
d_{65}						2.00	2.00
d_{54}					2.00	2.08	2.07
d_{43}				2.00	2.06	2.02	2.03
d_{32}			2.00	2.08	2.04	2.06	2.05
d_{21}		2.00	2.02	2.00	2.01	2.01	2.04
d_{11}	1.97	2.01	2.00	2.01	2.01	2.01	
d_{12}	0.46	0.46	0.46	0.46	0.46	0.46	
d_{23}	1.58	1.58	1.58	1.58	1.58	1.58	

OT position results in a large binding energy of 1.9 eV per Co atom. This energy is calculated by subtracting the total energy of the monolayer and the relaxed unpolarized C(111) surface from the energy of the hybrid system.[19] As a further test of the stability of the OT structure we have moved the Co top layer parallel to the surface allowing the Co atoms to relax laterally. In any case, it turns out that the atoms return to their original OT positions. To ease the following discussions we have labeled the C and Co layers of the system by C1, C2, and so on, as well as Co1, Co2, and so forth starting with $n=1$ *at both sides* of the interface.

Adsorption of cobalt in *hollow* sites, in which the Co atoms are located above the C atoms of the second substrate layer, turns out to be an unstable structure. In this configuration, the C atoms of the topmost substrate layer have an inappropriate sixfold coordination. As a result, this structure turns out to be 0.35 eV per Co atom less favorable than the OT configuration in which all C atoms on the top layer of the substrate are fourfold coordinated.

Cobalt atoms of additional adlayers adsorb in hcp bulk Co sites characteristic for a Co(0001) surface. The respective structure of the 2-Co:C(111) system is incorporated in Fig. 1. The Co atoms of the second adlayer are indicated by large open circles. In principle, it is also be possible to adsorb further cobalt adlayers in an fcc-like *ABC* stacking. It turns out, however, from our calculations that hcp stacking is about 50 meV per 1×1 unit cell more favorable in total energy than fcc stacking.

The calculated interlayer distances between neighboring layers in n-Co:C(111) hybrid systems with up to six Co adlayers are summarized in Table I. For example, d_{43} is the distance between Co adlayers Co4 and Co3. The last column of the table shows the interlayer distances between the first six Co layers of a Co(0001) surface.[22] Actually, for n-Co:C(111) systems d_{11} is the length of the Co-C interface bond and d_{23} is close to the bulk-bond length of diamond [see Fig. 1(b)]. There are a few general trends to be noted in Table I. First, the interlayer distances d_{21}, d_{11}, d_{12}, and d_{23} converge very quickly with increasing adlayer number. For more than one Co adlayer the length of the Co-C interface bond d_{11} turns out to be close to the respective interlayer distance $d_b=2.05$ Å in hcp bulk Co which is far from trivial. As a matter of fact, the carbon interlayer distances d_{12} and d_{23} are similar to the corresponding interlayer distances (0.51 and 1.54 Å, respectively) in bulk diamond. This implies a small impact of the Co adlayers on the structural properties of the substrate surface. In addition, the interlayer distance between the two top layers of each hybrid system is close to 2.00 Å and is thus about 0.05 Å smaller than the interlayer distance d_b in hcp bulk Co. This finding can be traced back to the lower coordination of the Co atoms on the topmost adlayer of the hybrid systems, as compared to that in hcp bulk Co. The interlayer distances at the Co(0001) surface, calculated for a 12 layer slab in the supercell (last column in Table I), quickly converge toward the Co bulk interlayer distance d_b, as one would expect. Comparing them with those of the $n=6$ hybrid system shows very close resemblance for the top five layers (first four values). Only the fifth interlayer distance $d_{21}=2.01$ Å in the $n=6$ hybrid system deviates from the value of 2.04 Å at the Co(0001) surface since it is markedly influenced by the C1 layer at the interface. This further corroborates the fast and efficient decoupling of all but the first adlayer from the substrate. Respective conclusions can be drawn for the other multilayer systems with $n<6$.

The second kind of hybrid systems suggested in this work contains n layers of Co adsorbed on a C(001) substrate. They are referred to as n-Co:C(001) systems. For one Co adlayer adsorbed on C(001) the most stable adsorption site of the Co atoms is a symmetric *bridge* site between neighboring C surface atoms, as indicated by the large filled (red) circles in Fig. 2. The latter together with the small (blue) circles (C atoms) indicate the structure of the corresponding one-adlayer system. In this case, the Co atoms reside in positions of an ideal diamond lattice on the first layer above the C(001) surface. Now they form two strong Co-C *pd* bonds across the interface which saturate all dangling bonds of the substrate surface. The binding energy per Co atom is 3.3 eV, referred to a free Co monolayer and the relaxed C(001) surface.[25] It is almost twice as large as the binding energy per Co atom in the 1-Co:C(111) system due to the two Co-C bonds per unit cell. Adsorption of Co in OT positions turns

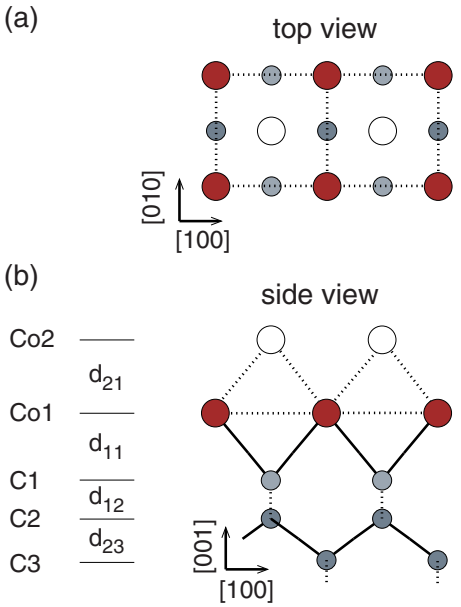

FIG. 2. (Color online) Top and side view of one and two Co layers on the C(001) surface (see text). For further details, see caption of Fig. 1.

out to be less favorable by 0.65 eV per Co atom and is, more importantly, unstable against lateral displacements of the Co atoms.

Our structure optimizations show that Co atoms of further adlayers adsorb in fcc bulk Co sites characteristic for a Co(001) surface. The large open circles in Fig. 2 indicate the respective sites of the Co atoms in the topmost adlayer of a 2-Co:C(001) system. The results of the structure optimizations for the n-Co:C(001) systems are summarized in Table II. Note that for the n-Co:C(001) systems the interlayer distance d_{11} is not equal to the length of the Co-C interface bonds [see Fig. 2(b)]. The interlayer distance of the two Co top layers of some 1.74 Å is about 0.04 Å smaller than the corresponding interlayer distance d_b=1.78 Å in fcc bulk Co. This inward relaxation, which is similar in size to that for the n-Co:C(111) systems discussed above, is also due to the lower coordination of the topmost Co adatoms in the hybrid systems, as compared to that in fcc bulk Co. The behavior of the interlayer spacings for a given adlayer number n as a function of adlayer number is very close to the one which we find for the clean Co(001) surface (see last column of Table II). The interlayer distances of the cubic Co(001) surface show a faster convergence, as compared to the hexagonal Co(0001) surface. The general behavior of the other structural properties in Table II is very similar to that discussed above for the n-Co:C(111) systems.

B. Electronic and magnetic properties

In this section, we present and discuss electronic and magnetic properties of the proposed n-Co:C(111) and n-Co:C(001) hybrid systems. We begin with one Co adlayer on the C(111) surface. Thereafter, we discuss the changes that occur for an increasing number of Co adlayers on C(111) and eventually proceed to the n-Co:C(001) systems.

1. Co on C(111)

As noted above, the energy optimized OT configuration of 1-Co:C(111) is characterized by the formation of one strong Co-C bond per unit cell. This leads to unique features in the associated electronic structure. Figure 3 shows the spin-resolved band structures and densities of states of one Co adlayer on C(111) in the energy region near the Fermi level. To ease the discussion we have superimposed the projected band structure (PBS) of bulk diamond (shaded areas) on the band-structure plots. There is one Co atom per unit cell in the top layer which has one 4s and five 3d states. It interacts predominantly with the one C atom per unit cell on the second layer having C 2p states. As a consequence, we find seven bands in the projected band gap which result from the partially hybridized Co 4s and Co 3d, as well as C 2p states. They are only partially occupied. As a result, the 1-Co:C(111) hybrid system is metallic which becomes also very clear from the densities of states [see Fig. 3(c)]. Comparing the band structures of the 1-Co:C(111) system for spin-up [Fig. 3(a)] and spin-down [Fig. 3(b)] electrons, we first note that they show only a weak spin splitting. Furthermore, the dispersion of the bands is almost identical for both spin polarizations. Therefore, we restrict ourselves to the analysis of the majority-spin bands at this point. Based on a Mulliken analysis, we have marked the bands originating from Co d states with a major contribution from C p states that are mainly localized at the topmost C atoms by thick lines in Fig. 3. Actually, these states consist of a strong mix-

TABLE II. Interlayer distances d_{ij} (in Å) between neighboring atomic layers i and j for n-Co:C(001) hybrid systems with n varying from 1 to 6. For further details, see caption of Table I.

	1	2	3	4	5	6	Co(001)
d_{65}						1.74	1.73
d_{54}					1.74	1.80	1.78
d_{43}				1.73	1.80	1.78	1.77
d_{32}			1.74	1.80	1.79	1.79	1.77
d_{21}		1.73	1.80	1.77	1.78	1.77	1.77
d_{11}	1.43	1.52	1.51	1.51	1.51	1.51	
d_{12}	0.84	0.84	0.84	0.84	0.84	0.84	
d_{23}	0.91	0.91	0.91	0.91	0.91	0.91	

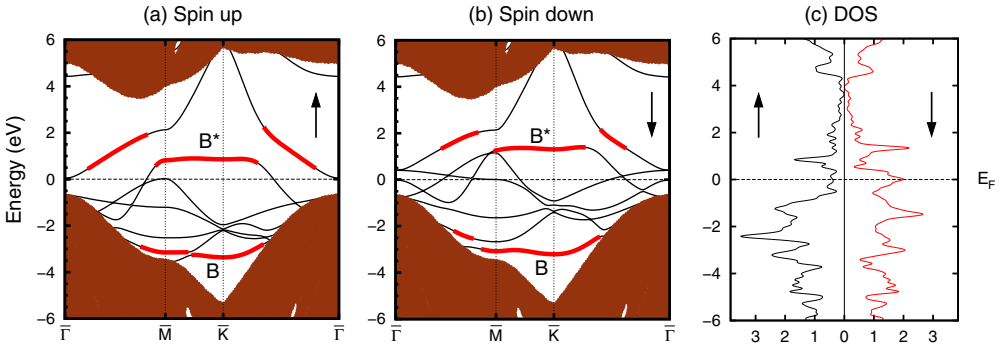

FIG. 3. (Color online) Band structures of 1-Co:C(111) for (a) spin-up and (b) spin-down electrons. Respective spin-resolved densities of states are shown in (c). The shaded areas represent the projected band structure of bulk diamond. The band energies and state densities are referred to E_F which we define as the zero of energy (horizontal dashed lines). The band sections highlighted by thick lines originate from Co d states that have strong admixtures of C p states which are mainly localized at the atoms of the topmost C layer.

ture of Co $d_{3z^2-r^2}$ and C p_z orbitals giving rise to the formation of an occupied bonding band B and a mostly unoccupied antibonding band B^*. This particular mixture of Co $d_{3z^2-r^2}$ and C p_z states gives rise to strong covalent Co-C bonds which are oriented perpendicular to the interface [see Fig. 1(b)].

To further illustrate this point, Fig. 4 shows charge density contours for the B and B^* states at the high-symmetry point $\bar{K}$ of the Brillouin zone. State B exhibits a large accumulation of charge density between the Co adlayer and substrate C top layer atom (filled large red and small blue circle, respectively, in the left panel of Fig. 4) implying a strong covalent bond between the two atoms. In contrast, the charge density of the unoccupied state B^* has a nodal plane between the Co and C atom emphasizing its antibonding character.

The remaining bands in the gap energy region of Fig. 3 below E_F can be attributed to states that are predominantly localized at the Co adlayer. They are already present in the band structure of an isolated Co monolayer and are not a specific feature of the 1-Co:C(111) hybrid system, therefore. Additional important information about the system can be inferred from the spin-resolved densities of states in Fig. 3(c). As was to be expected from the spin-resolved band structures, two similar densities of states result which are shifted relative to each other within the energy range from −5 to +4 eV.

Adding further Co adlayers to the system rapidly leads to an increase in the number of bands near the Fermi level with adlayer number n so that the band structure becomes very congested. The slab bands originating from the Co adlayers start to build up the PBS of bulk Co. Superimposing it onto the PBS of bulk diamond leaves only relatively small empty pockets in the respective joint PBS. They define the energy regions where bands of truly localized Co-C interface and Co(0001) surface states can appear. Actually, for all investigated n-Co:C(111) hybrid systems with $n \geq 2$, which also clearly turn out to be metallic, we find the characteristic B and B^* bands near −3 and around +1 eV originating from the Co-C interface bonds, as discussed in the context of Fig. 3.

Next, we analyze the magnetic properties of n-Co:C(111) hybrid systems. The magnetic moments per atom on a given layer for n from 1 to 6, as resulting from our calculations are presented in Table III together with respective relative and absolute spin polarizations at E_F on the Co1 and C1 layer at the interface and at the Co top layer of each hybrid system. For reference, the magnetic moments, as well as the relative spin polarizations at E_F for hexagonal and cubic bulk Co, the Co(0001) and Co(001) surfaces and a hexagonal, as well as a cubic Co monolayer are given in Table IV. We note in passing that the magnetic moments in Table IV are smallest for the bulk crystals and largest for the monolayers. This is a direct consequence of the decreasing coordination of the Co atoms when proceeding from the bulk over the surface to the monolayer. Their properties become more and more atomic-like along the way. Our μ_{bulk} values of 1.62 and 1.68μ_B for hcp and fcc Co, respectively, are in good agreement with the values of 1.61μ_B, as reported in Ref. 27 for hcp Co, as well as 1.60 and 1.66μ_B, as reported in Refs. 27 and 28 for fcc Co, respectively.

A number of interesting trends are to be observed in Table III. First of all, the formation of local magnetic moments is largely limited to the Co layers whereas the C layers remain essentially unmagnetized. Second, we observe that not only

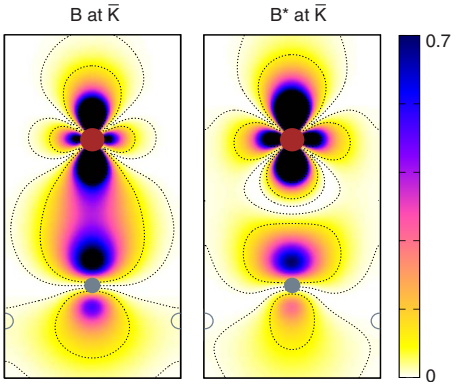

FIG. 4. (Color online) Charge density contours (in Å^{-3}) for the bonding (B) and antibonding (B^*) state at the $\bar{K}$ point for the 1-Co:C(111) system. Large and small filled circles mark Co and C atoms, respectively, that are located in the drawing plane. The charge densities are plotted in the [1000]-[0001] plane containing the Co and C atom at the interface.

TABLE III. Magnetic moment μ per atom and layer unit cell (in μ_B), as well as relative (in %) and absolute (in 1/eV) spin polarization $\zeta(E_F)$ and $\zeta^{\mathrm{abs}}(E_F)$ per layer unit cell for n-Co:C(111) hybrid systems.

Layer	1	2	3	4	5	6
$\mu_{\mathrm{Co}6}$						1.77
$\mu_{\mathrm{Co}5}$					1.76	1.62
$\mu_{\mathrm{Co}4}$				1.78	1.60	1.61
$\mu_{\mathrm{Co}3}$			1.75	1.63	1.60	1.63
$\mu_{\mathrm{Co}2}$		1.76	1.51	1.56	1.53	1.56
$\mu_{\mathrm{Co}1}$	0.96	1.26	1.07	1.23	1.11	1.19
$\mu_{\mathrm{C}1}$	−0.09	−0.10	−0.13	−0.13	−0.13	−0.13
$\mu_{\mathrm{C}2}$	0.02	0.03	0.03	0.03	0.03	0.03
$\zeta_{\mathrm{Co}\,n}$	−69	−62	−77	−76	−80	−73
$\zeta_{\mathrm{Co}1}$	−69	−51	−64	−50	−64	−41
$\zeta_{\mathrm{C}1}$	−13	+6	+55	+31	+38	+42
$\zeta^{\mathrm{abs}}_{\mathrm{Co}\,n}$	−1.56	−0.31	−1.11	−0.75	−0.98	−0.76
$\zeta^{\mathrm{abs}}_{\mathrm{Co}1}$	−1.56	−0.24	−1.09	−0.54	−0.84	−0.47
$\zeta^{\mathrm{abs}}_{\mathrm{C}1}$	−0.01	−0.01	0.06	0.03	0.04	0.05

for one Co adlayer but for all cases with n from 1 to 6, the magnetic moment of the Co atoms at the interface ($\mu_{\mathrm{Co}1}$) is considerably smaller than the respective value of bulk Co ($1.62\mu_B$) or at the Co(0001) surface layer ($1.76\mu_B$). In particular, it is also much smaller than the magnetic moment of a free-standing hexagonal Co monolayer ($1.87\mu_B$). The large magnetic moment of a Co monolayer results mainly from the splitting of Co $d_{3z^2-r^2}$ derived spin-up and spin-down bands, which have a rather flat dispersion in a large region of the surface Brillouin zone along the $\overline{\Gamma M}/2-\bar{M}$, $\bar{M}-\bar{K}$, and $\bar{K}-\overline{K\Gamma}/2$ lines. The band structure of the hexagonal Co monolayer is not shown for brevity. While the $d_{3z^2-r^2}$ spin-up band in this band structure is completely occupied, a flat region of the $d_{3z^2-r^2}$ spin-down band is unoccupied in about half of the Brillouin zone. This fact leads to a contribution of about $1\mu_B$ to the magnetic moment of each Co atom in the monolayer. For 1-Co:C(111), however, the coupling between the Co $d_{3z^2-r^2}$ and C p_z orbitals gives rise to the bands B and B^*, as discussed above, whose occupation is almost the same for spin-up and spin-down electrons, respectively. These bands do not contribute to the magnetization and the magnetic moment of the Co atoms at the interface is about $1\mu_B$ lower than in a free monolayer, therefore. The covalent bonding of the Co to the C interface layer thus quenches the magnetic moment on the Co1 layer to a considerable extent.

TABLE IV. Magnetic moment per atom (in μ_B) and relative spin polarization ζ at E_F (in %) for hexagonal bulk Co, the Co(0001) surface layer, and a hexagonal Co monolayer, as well as for fcc bulk Co, the Co(001) surface layer and a fcc Co monolayer.

	hex	fcc
μ_{bulk}	1.62	1.68
μ_{surf}	1.76	1.92
μ_{mono}	1.87	2.05
ζ_{bulk}	−80	−75
ζ_{surf}	−80	−78
ζ_{mono}	−71	−83

For more than one Co adlayer the local magnetic moments increase almost monotonously when going from the interface to the surface. At the topmost adlayer the magnetic moment per Co atom is close to that on a Co(0001) surface layer ($1.76\mu_B$).

Table III also shows relative spin polarizations per layer unit cell at E_F for the Co1 and C1 layers at the interface and for the top layer Co n of the six n-Co:C(111) systems. A striking feature of these spin polarizations is the variation in its value for systems with different adlayer numbers. In the 1-Co:C(111) system, the cobalt adlayer (Co1) is strongly spin polarized ($\zeta_{E_F}=69\%$). Addition of another Co adlayer reduces the spin polarization to 51% for the 2-Co:C(111) system. For more Co adlayers the spin polarization starts to oscillate with respect to the number of adlayers. In general, the systems with an odd number of adlayers show a larger spin polarization of 64–69 % whereas systems with an even number of adlayers are less spin polarized (41–51 %). Most importantly, the relative spin polarization on the Co surface layer Co n of the adlayer systems with $n=2-6$ is considerably larger than that on the respective Co1 interface layer. Actually, for the systems with $n=4-6$ it is close to the relative spin polarization on the surface layer ($\zeta_{\mathrm{surf}}=80\%$) of the Co(0001) surface. The relative spin polarization on carbon interface layer C1 also shows strong variations with adlayer number. This peculiar behavior of the relative spin polarizations is closely correlated with subtle changes in the electronic structure around E_F for different numbers of Co adlayers. It changes very sensitively as a function of n and as a function of energy (not shown for brevity sake). The energetic position of the relevant peak in the DOS for spin-down electrons near E_F varies strongly with adlayer number. While the DOS of the spin-up electrons is comparatively small at E_F for all investigated Co coverages [see Fig. 3(c) for that matter], the spin-down DOS at E_F changes more strongly

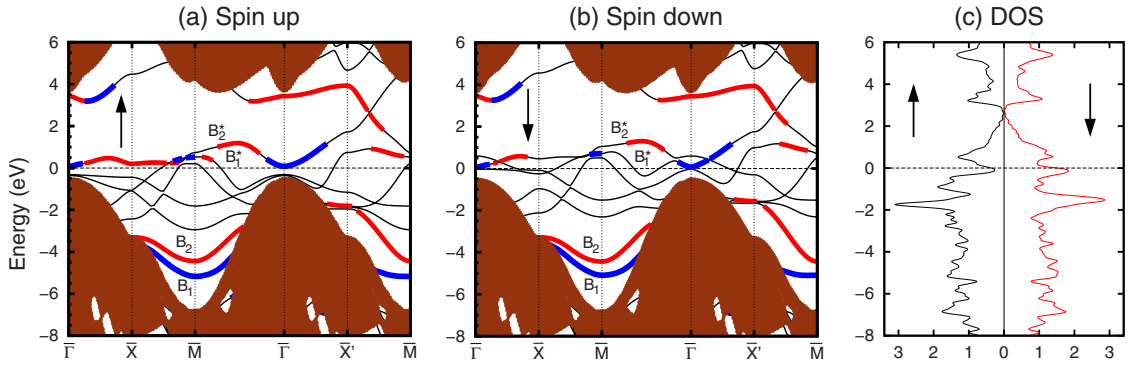

FIG. 5. (Color online) Band structures for (a) spin-up and (b) spin-down electrons and (c) spin-resolved densities of states for 1-Co:C(001). The shaded areas represent the PBS of bulk diamond. For further details, see caption of Fig. 3.

with coverage. For 1-Co:C(111) the flat bands originating from the Co d_{xz} and d_{yz} orbitals give rise to a peak in the spin-down DOS around E_F resulting in the large spin polarization of 69% on layer Co1. Adsorption of a second Co layer leads to an even stronger spin splitting of the related bands and therefore to a larger upward shift of the spin-down bands with respect to E_F. As a result, the above-mentioned peak in the spin-down DOS is now located at about 1 eV above E_F while a minimum of the spin-up DOS exists close to E_F. This gives rise to a smaller spin polarization of about 50% on layer Co1. Adsorption of further Co layers slightly increases the spin splitting and the peak in the spin-down DOS is shifted to 1.2 eV above E_F, thereby. Concomitantly, the DOS at E_F is increased. These subtle changes in the electronic structure result in a large sensitivity of the spin polarizations with respect to the number of adsorbed Co layers. The relative spin polarization on the carbon interface layer C1 is also fairly large for the first three hybrid systems with $n=1-3$. It should be noted, however, that the respective *absolute* spin polarizations on the C1 interface layers are much smaller than those on the related Co1 interface layers.

2. Co on C(001)

The electronic structure of n-Co:C(001) hybrid systems is slightly more intricate since there are two Co-C bonds at the interface in this case. By symmetry [see Fig. 2(b)] it is to be expected that the two Co-C interface bonds are now mainly formed by linear combinations of Co $d_{3z^2-r^2}$ and Co d_{zx}, as well as C p_x and C p_z states. Here, we have identified the x direction with the [100] crystal axis. Again, we first discuss the band structure and magnetic properties for one Co adlayer. The band structure for 1-Co:C(001) contains eight bands within the projected fundamental gap as can be seen in Figs. 5(a) and 5(b). This system is metallic, as well. The bands for spin-up and spin-down electrons are again rather similar whereby the spin-down bands are slightly shifted toward higher energies. Also in this case we restrict ourselves to a discussion of the spin-up bands. The interaction between the Co adlayer and the C(001) substrate now leads to two bonding (B_1 and B_2) and two antibonding (B_1^* and B_2^*) bands since there are two Co-C interface bonds per unit cell. An analysis of the symmetry of these bands shows that the states giving rise to the bands B_1 and B_1^* [shown in blue in Figs. 5(a) and 5(b)] have large contributions from Co d_{zx} and C p_z orbitals. On the other hand, the states giving rise to the bands B_2 and B_2^* (shown in red) can be ascribed to a superposition of Co $d_{3z^2-r^2}$ and C p_x orbitals.

To further highlight the character of the respective states we present in Fig. 6 the associated charge densities at the $\bar{M}$ point. There is a strong localization of the charge density between the Co and the two C atoms for the B_1 and B_2 bonding states. The Co and C orbitals thus form strong covalent bonds also in the 1-Co:C(001) system. This leads to the rather high binding energy of 3.3 eV per Co adatom. The corresponding antibonding states B_1^* and B_2^* exhibit large charge density contributions above the Co adlayer atoms resulting in a reduced screening in the spatial regions between

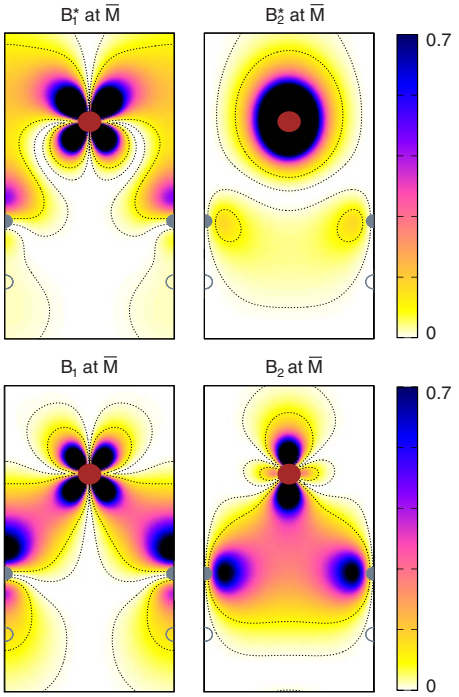

FIG. 6. (Color online) Charge densities of the bonding (B_1 and B_2) and antibonding (B_1^* and B_2^*) states of the 1-Co:C(001) system at the $\bar{M}$ point of the Brillouin zone. The charge densities are plotted in the [100]-[001] plane containing the Co and the two C atoms at the interface.

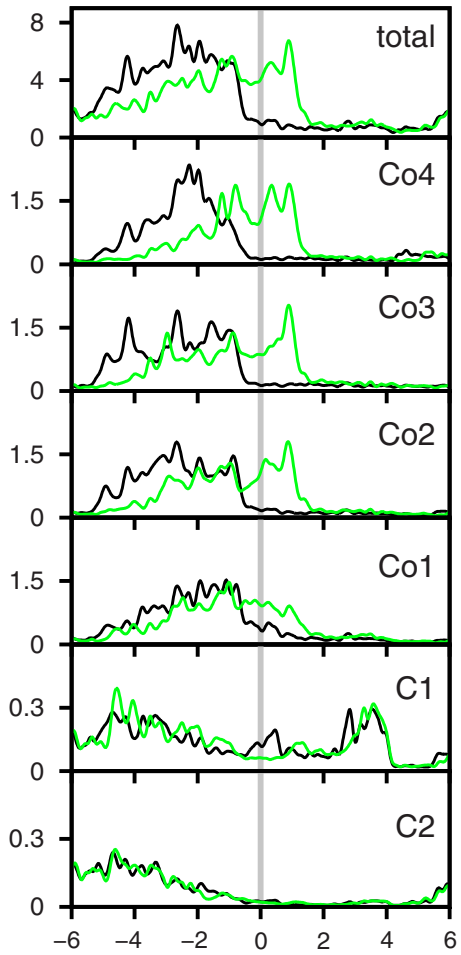

FIG. 7. (Color online) Layer-resolved densities of states for spin-up (black lines) and spin-down (green lines) electrons of the 4-Co:C(001) system. Note that the scales for the total DOS, the Co-layer DOSs, and the C-layer DOSs are different.

the Co and C atoms in close similarity with the behavior observed for the 1-Co:C(111) system. We note that the B_2^* state at the $\bar{M}$ point, in particular, shows a rather circular charge distribution which can be attributed to the strong mixture of orbitals with respective symmetries.

Next, we discuss n-Co:C(001) systems with more than one Co adlayer. Since the band structures for these systems become very complex and congested with increasingly larger adlayer numbers, as well, we address layer-resolved DOSs (LDOSs) instead. Figure 7 shows the LDOSs of a 4-Co:C(001) hybrid system as an example. Note, that different density scales are used for the total DOS, the LDOS on the Co layers and the LDOS on the C layers. The LDOS on the Co layers is much larger than on the C layers due to the contributions of the Co d states. One can immediately see that the LDOS for the spin-up (black lines) and spin-down (green lines) electrons localized at the Co atoms on the topmost three layers are shifted near the Fermi energy with respect to each other by about 2 eV. This effect is strongly reduced for the Co1 layer at the interface. On the first carbon layer C1, there is an appreciable LDOS within the gap energy region due to formation of the Co-C pd states. On the lower C layers, however, the insulating behavior of diamond is restored. Already on the second carbon layer C2 the fundamental gap is almost free from states. Moreover, this layer is almost completely unpolarized as was the case for the C2 layer in the n-Co:C(111) systems.

The resulting magnetic properties for up to six Co adlayers on C(001) are summarized in Table V. The general trends in magnetization are quite similar to the ones discussed above for the n-Co:C(111) systems. In detail, however, there are some marked differences. The additional Co-C bond per unit cell, e.g., has significant consequences for the magnetic properties of the respective interface. For 1-Co:C(001) the magnetic moment of the Co adlayer atoms is only $0.42\mu_B$ and thus only about half as large as for the 1-Co:C(111) system. Thus, the two covalent Co-C bonds across the interface quench the magnetic moment on the interface layer Co1 in this case even considerably stronger. When more Co layers are added, μ_{Co1} remains also fairly small since the respective B_1, B_2 and B_1^*, B_2^* bands contribute only marginally to the magnetization in all cases. For more than one adsorbed Co layer the local magnetic moment per Co atom in the topmost layer converges very quickly to $1.92\mu_B$ which is precisely the magnetic moment of a Co atom at the top layer of the Co(001) surface (cf. Table IV). The magnetic moments on the Co adlayers in the n-Co:C(001) systems are larger than those for the n-Co:C(111) systems and the Co(0001) surface, respectively, due to the lower coordination of the top layer Co atoms in the n-Co:C(001) systems. The C layers behave in the same way as in the case of n-Co:C(111) and show again a small antiparallel magnetic moment on the first and an almost completely vanishing moment on the second C layer.

For all n-Co:C(001) hybrid systems the B_1, B_2 and B_1^*, B_2^* bands originating from the Co-C interface bonds contribute only slightly to the spin polarization at E_F. As a result, e.g., the spin polarization for one Co adlayer on C(001) of 64% is again smaller than the polarization of the related free-standing fcc Co monolayer (83%). Likewise, for two or more Co adlayers the polarization at the Co interface layer is somewhat smaller than in fcc bulk Co where it amounts to 75% (cf. Table IV). The relative spin polarization on the surface layer Co n of the n-Co:C(001) systems is once again much larger than that on the respective Co1 interface layers. For the systems with $n \geq 3$ it approaches $\zeta_{\mathrm{surf}}=78\%$ of the Co(001) surface. For the n-Co:C(001) hybrid systems, we observe fairly large relative spin polarizations on most of the carbon interface layers C1 in the different hybrid systems but the absolute spin polarizations on these layers are once again much smaller than on the cobalt interface layers Co1.

IV. SUMMARY

In summary, we have investigated structural, electronic, and magnetic properties of lattice-matched metal-semiconductor hybrid systems in the framework of spin-density-functional theory employing the generalized gradient approximation. They consist of one up to six Co adlayers on C(111) and C(001) substrate surfaces.

Exploring several adsorption sites for Co atoms on the first adlayer by total-energy minimization, we have found

TABLE V. Magnetic moment μ per atom and layer unit cell (in μ_B), as well as relative (in %) and absolute (in 1/eV) spin polarization $\zeta(E_F)$ and $\zeta^{\mathrm{abs}}(E_F)$ per layer unit cell for n-Co:C(001) hybrid systems.

Layer	1	2	3	4	5	6
$\mu_{\mathrm{Co}6}$						1.92
$\mu_{\mathrm{Co}5}$					1.92	1.62
$\mu_{\mathrm{Co}4}$				1.93	1.62	1.68
$\mu_{\mathrm{Co}3}$			1.93	1.62	1.67	1.67
$\mu_{\mathrm{Co}2}$		1.92	1.57	1.65	1.63	1.65
$\mu_{\mathrm{Co}1}$	0.42	0.94	0.86	0.90	0.89	0.91
$\mu_{\mathrm{C}1}$	−0.05	−0.07	−0.07	−0.07	−0.07	−0.07
$\mu_{\mathrm{C}2}$	0.01	0.01	0.01	0.01	0.01	0.01
$\zeta_{\mathrm{Co}\,n}$	−64	−70	−79	−80	−76	−78
$\zeta_{\mathrm{Co}1}$	−64	−36	−54	−46	−48	−48
$\zeta_{\mathrm{C}1}$	−21	+45	+24	+31	+38	+23
$\zeta^{\mathrm{abs}}_{\mathrm{Co}\,n}$	−1.11	−0.78	−1.16	−0.94	−1.00	−0.97
$\zeta^{\mathrm{abs}}_{\mathrm{Co}1}$	−1.10	−0.36	−0.94	−0.58	−0.73	−0.63
$\zeta^{\mathrm{abs}}_{\mathrm{C}1}$	−0.02	0.07	0.05	0.06	0.08	0.04

favorable adsorption configurations for both substrate surfaces which lead to a complete saturation of all surface dangling bonds. In the case of the C(111) surface each Co atom adsorbs in on top position while on C(001) it adsorbs in a symmetric bridge position above neighboring carbon surface atoms. Further Co layers reside in these systems in lattice sites of a continued hcp or fcc bulk lattice, respectively. In either case, the structural properties of the underlying relaxed diamond surfaces are hardly affected by the Co adlayers.

The strong covalent *pd* bonds between the Co and C atoms formed at the interfaces give rise to characteristic bands of bonding and antibonding states that are energetically located in the projected fundamental gap of the respective diamond substrate surfaces. These states have a strong influence on the magnetic properties of the systems. The local magnetic moments of the Co atoms on the interface layer are significantly reduced, as compared to their respective bulk or surface values. For all investigated systems they increase, however, from the Co-C interface to the Co surface of the hybrid systems eventually approaching the surface-layer magnetic moments of the clean Co(0001) and Co(001), respectively. We find high spin polarizations at the Fermi level of 69% and 64% for one Co adlayer on C(111) and C(001), respectively. Interestingly, the spin polarization at E_F depends sensitively on the number of Co adlayers.

ACKNOWLEDGMENTS

We would like to thank J. Wieferink for useful discussions. This work was supported by a grant of computer time on the JUMP computer of the John von Neuman Institute for Computing (NIC) of the Forschungszentrum Jülich (Germany) under Contract No. HMS08/2961.

*bernd.staerk@uni-muenster.de

[1] I. Žutić, J. Fabian, and S. Das Sarma, Rev. Mod. Phys. **76**, 323 (2004).
[2] S. Datta and B. Das, Appl. Phys. Lett. **56**, 665 (1990).
[3] M. Hortamani, H. Wu, P. Kratzer, and M. Scheffler, Phys. Rev. B **74**, 205305 (2006).
[4] L. Sacharow, M. Morgenstern, G. Bihlmayer, and S. Blügel, Phys. Rev. B **69**, 085317 (2004).
[5] M. Zwierzycki, K. Xia, P. J. Kelly, G. E. W. Bauer, and I. Turek, Phys. Rev. B **67**, 092401 (2003).
[6] A. Fert and H. Jaffrès, Phys. Rev. B **64**, 184420 (2001).
[7] V. M. Karpan, G. Giovannetti, P. A. Khomyakov, M. Talanana, A. A. Starikov, M. Zwierzycki, J. van den Brink, G. Brocks, and P. J. Kelly, Phys. Rev. Lett. **99**, 176602 (2007).
[8] S. M. Shapiro and S. C. Moss, Phys. Rev. B **15**, 2726 (1977).
[9] R. N. Grass and W. J. Stark, J. Mater. Chem. **16**, 1825 (2006).
[10] S. Fox and H. J. F. Jansen, Phys. Rev. B **60**, 4397 (1999).
[11] S. M. Sze, *Physics of Semiconductor Devices* (Wiley, New York, 1981).
[12] J. P. Perdew, K. Burke, and M. Ernzerhof, Phys. Rev. Lett. **77**, 3865 (1996).
[13] L. Kleinman and D. M. Bylander, Phys. Rev. Lett. **48**, 1425 (1982).
[14] D. R. Hamann, Phys. Rev. B **40**, 2980 (1989).
[15] S. G. Louie, S. Froyen, and M. L. Cohen, Phys. Rev. B **26**, 1738 (1982).
[16] As decay constants we use 0.18, 0.84, 2.97, and 10.02 for Co and 0.25, 0.87, and 3.60 for C atoms (in atomic units), while a decay constant of 0.35 is employed for the saturating hydrogen atoms.
[17] J. Wieferink, P. Krüger, and J. Pollmann, Phys. Rev. B **74**, 205311 (2006).
[18] H. J. Monkhorst and J. D. Pack, Phys. Rev. B **13**, 5188 (1976).

[19] If we refer the binding energy to the total energy of the Co monolayer and the 2×1 reconstructed C(111) surface it still amounts to 1.15 eV. The difference of 0.78 eV is the energy gain (per 1×1 cell) due to the 2×1 reconstruction, as resulting from our calculations. It is close to the respective value of 0.83 eV, as reported by Scholze *et al.* (Ref. 20). Respective reconstruction energies resulting from LDA and GGA calculations differ only slightly (Ref. 21).

[20] A. Scholze, W. G. Schmidt, and F. Bechstedt, Phys. Rev. B **53**, 13725 (1996).

[21] M. Saito, A. Oshiyama, and Y. Miyamoto, Phys. Rev. B **57**, R9412 (1998).

[22] Our corresponding contractions and expansions, as resulting for the theoretical Co lattice constants are in very good accord with respective results of a former pseudopotential calculation (Ref. 23) and experimental data (Ref. 24).

[23] L. G. Wang, E. Y. Tsymbal, and S. S. Jaswal, Phys. Rev. B **70**, 075410 (2004).

[24] J. Lahtinen, J. Vaara, T. Vaara, K. Kauraala, P. Kaukasoina, and M. Lindroos, Surf. Sci. **425**, 90 (1999).

[25] If we refer the binding energy in this case to the total energy of the Co monolayer and the 2×1 reconstructed C(001) surface it is still 1.84 eV. The large difference of 1.46 eV resulting from our calculations is the energy gain (per 1×1 cell) due to the 2×1 dimer reconstruction. This energy gain happens to be identical to the respective value of 1.46 eV, as reported by Steckel *et al.* (Ref. 26).

[26] J. A. Steckel, G. Kresse, and J. Hafner, Phys. Rev. B **66**, 155406 (2002).

[27] E. G. Moroni, G. Kresse, J. Hafner, and J. Furthmüller, Phys. Rev. B **56**, 15629 (1997).

[28] J.-H. Cho and M. Scheffler, Phys. Rev. B **53**, 10685 (1996).